Građevinski materijali i konstrukcije
Building Materials and Structures
journal homepage: www.dimk.rs

doi: 10.5937/GRMK2104225I UDK: 624.012.45.042.7
Original scientific paper

Shake table test of RC walls' coupling provided by slabs

T. Isaković *[1)], M. Gams[1)], A. Janevski[1)], Z. Rakićević[2)], A. Bogdanović[2)], G. Jekić[2)], K. Kolozvari[3)], J. Wallace[4)], M. Fischinger[1)]

[1)] *University of Ljubljana, Faculty of Civil and Geodetic Engineering, Ljubljana, Slovenija*
[2)] *Institute of Earthquake Engineering and Engineering Seismology IZIIS, Skopje, North Macedonia*
[3)] *California State University, Fullerton,USA*
[4)] *University of California, Los Angeles, USA*

Article history

Received: 25 October 2021
Received in revised form: 12 November 2021
Accepted: 20 November 2021
Available online: 30 December 2021

Keywords

RC coupled walls,
Shake table test,
Floor-to-piers interaction,
Large scale experiment

ABSTRACT

When designed to the seismic load effects, reinforced concrete walls connected by slabs without coupling beams are usually considered cantilever walls. Several recent studies indicated that slabs themselves could provide strong coupling in some cases, and the walls could respond differently from cantilever walls. To study the slab-to-wall piers interaction, a shake table test of the half-scale three-story specimen was conducted within HORIZON 2020 SERA-TA project. The specimen consisted of four rectangular walls linked by three slabs. It was subjected to a series of seismic excitations of increasing intensity. In the last three tests, the nonlinear response of the slabs and wall piers was observed.

At the strong seismic excitations, one pier was subjected to strong tensile, while the adjacent pier was subjected to strong compression forces. The crack pattern of piers was asymmetric and different from the cross-shaped damage pattern, typical for cantilever walls.

The coupling of wall piers provided by slabs was considerably stronger than it was expected. The share of the overturning moment resisted by the frame action induced by the slabs was more than 50%. All slabs were fully activated and significantly damaged. Their damage was primarily flexural. The effective width of slabs was equal to their total width.

1 Introduction

During the seismic design of RC walls connected only by slabs (without coupling beams), experienced engineers typically consider them as cantilever walls. The slabs are considered rigid diaphragms. Their bending and shear stiffness are neglected, assuming they are small compared to the wall's stiffness. It is also assumed that the slab's flexural capacity is small compared to the bending capacity of the wall.

Following the previous assumptions, a hinged connection between piers and slabs are considered in the numerical model. The response mechanism of such a model to a horizontal load is shown in Figure 1a. The wall piers having the same properties are subjected to equal bending moments. There are no axial forces in piers due to the horizontal load.

However, in some cases, such a numerical model is not accurate enough, and the assumptions used to formulate it are less acceptable. The stiffness of the slabs is inversely proportional to the third power of the opening's width between piers. The stiffness of the walls is inversely proportional to the third power of the wall height. In some cases, the opening length is significantly smaller than the height of the walls (e.g. in the prototype of the tested specimen, the opening length is 1 m and the height of the wall is 9 m – see Section 2). Consequently, the ratio of the slab's stiffness and the stiffness of the wall piers is significantly larger than it is typically assumed in the traditional models. Moreover, the bending capacity of the slabs can also be considerably larger than it is generally expected and cannot be neglected. It depends on the effective width of the slabs, which is in some cases significantly larger than that assumed in the traditional design (this will be demonstrated later in the text).

Following the previous observations, it can be concluded that the slabs can provide significantly stronger coupling of wall piers than it is typically expected. When the stronger coupling is provided, the response of the piers and the entire building (see Figure1b) is significantly different from the response of an assembly of the cantilever walls. Since the bending capacity of slabs is not negligible, the corresponding shear forces induce the additional axial forces to wall piers.

* Corresponding author:
E-mail address: tatjana.isakovic@fgg.uni-lj.si

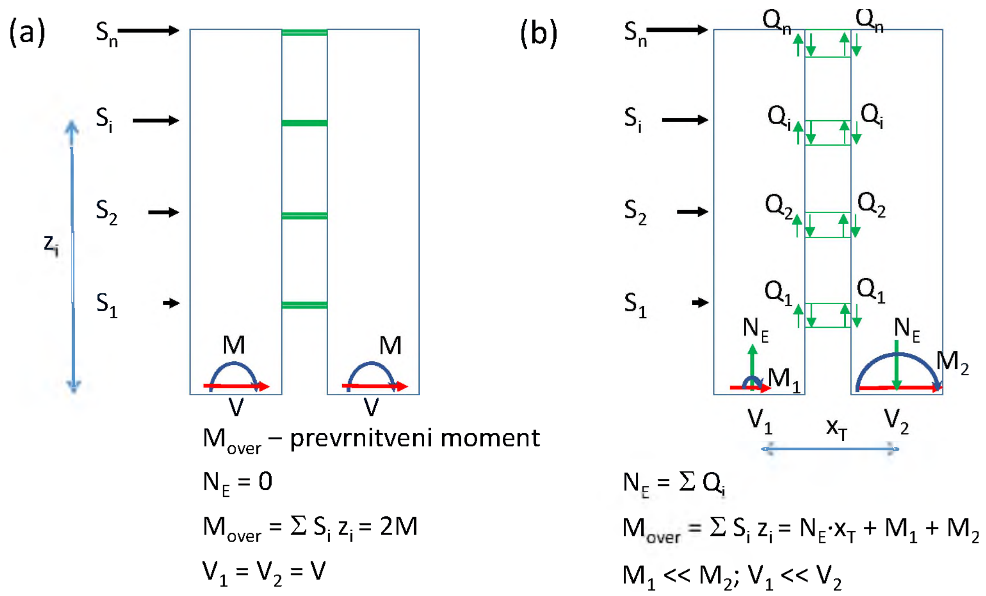

Figure 1. Resisting mechanisms: a) cantilever walls (very weak coupling), b) coupled walls (significant coupling of wall piers)

These forces cause the change of the stiffness as well as the strength of piers. The stiffness and strength of pier subjected to tensile seismic forces can be considerably smaller than the stiffness and the strength of piers subjected to compression. Due to stiffness changes, significant redistributions of demand between piers could occur in the nonlinear range. When these redistributions are disregarded in the design, considerable damage and even failure of piers can occur.

Experiments (e.g. [1], [2], [3]) proved that the forces in piers subjected to compression could be even doubled compared to the results of the elastic analysis. Therefore, even the sophisticated elastic shell numerical models, the use of which is rapidly increasing in practice, cannot be the solution to the problem.

Previous observations were confirmed during the earthquakes in Chile (2010) and New Zealand (2010, 2011) ([4], [5], [6]). The damage was particularly severe in higher buildings, where the buckling and the rupture of the longitudinal boundary reinforcement and the shear damage of piers were observed. One of the reasons for such damage is the inability of elastic models to consider the variable interaction between piers and floors.

Similar conclusions were obtained at UL FGG based on the shake table experiment of a typical European coupled wall (Figure2). This wall consisted of two non-planar wall piers ("T" shaped piers) connected by five slabs and five diagonally reinforced beams [1]. It was found that due to the interaction between beams and slabs, the bending strength of floors can be considerably larger than expected (determined using standard procedures). Consequently, the wall piers were considerably more coupled than it was predicted. The strong coupling resulted in brittle shear failure of wall piers.

The traditional assumption that the slab alone (without beams) cannot provide considerable coupling of wall piers has been recently called into question by several experiments and analytical studies (e.g. [7], [8]). In [7] (Figure 3), it was shown that even very thin slabs without beams could provide significant coupling of wall piers. The response of a seven-story rectangular wall was tested. It was connected to the perpendicular stabilizing wall only by slabs to avoid their interaction. To additionally minimize the coupling effect, slabs were slotted at the connection with the walls. They were only 5 cm thick at the slot (see Figure3b). Considerable shear forces were generated along the whole length of the slots, resulting in the substantial increase of the axial force in the tested wall. The bending moments and shear forces in the wall were also increased due to the induced axial forces.

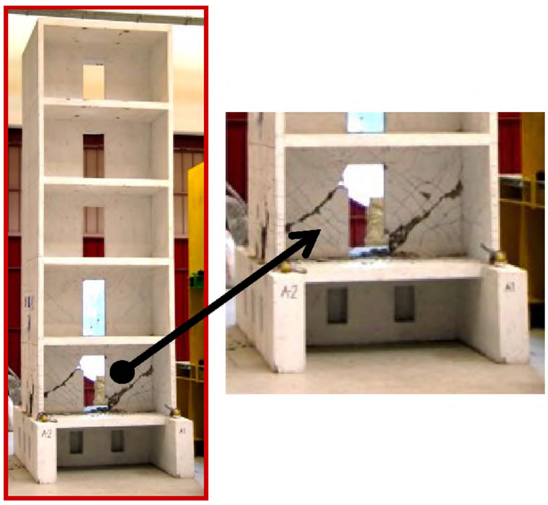

Figure 2. The brittle failure of the non-planar coupled walls tested at the shaking table

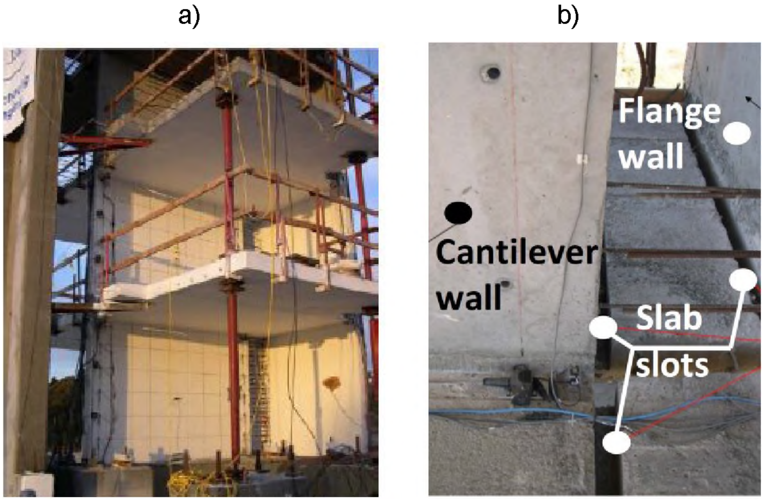

Figure 3. Cantilever RC wall tested at shake table at UCSD:
a) the wall and "gravity columns", used to support the slab and provide stability in the direction perpendicular to the wall plane
b) the slab slots (courtesy Panagiotou MM et al. [7])

The conclusions of this study demonstrate the essential subject of the research presented in this paper. The assumption that slabs due to the relatively small moment of inertia cannot significantly couple the wall piers and that connections between piers and floors can be represented by hinges with zero bending moments is inadequate for certain wall configurations. In such cases, the connections should be represented by plastic hinges, where the moment capacity depends on the slab's flexural strength. The bending moment corresponding to the flexural strength of the slab can be significant in all cases where the considerable effective width of the slab is activated. The shear forces in the slab corresponding to the flexural strength of the slab induce the variable axial forces in piers and can qualitatively change the response of the wall piers and the entire structure.

2 Description of the specimen, excitations and instrumentation

2.1 The geometry of the specimen

A shake table experiment of the half-scale three-story specimen consisting of four RC walls connected only by slabs (without any beams) was conducted (see Figures 4 and 5). To get as realistic as possible information about the slabs-to-walls interaction, the maximum possible size of the specimen was selected, considering the limitations of the shake table regarding the overturning moment (about 500 kNm). Scale factors considered in the design of the specimen are summarized in Table 1.

The main goal of the experiment was to obtain information about the varying floor-to-wall interaction at different levels of the response, particularly in the nonlinear range. Thus, the proper balance between the realistic size (strength) of the structural elements and the limitations of the shake table had to be found. The selected height of the walls' cross-section (75 cm) enabled the yielding of the walls when they were subjected to the maximum possible intensity of the seismic load limited by the performances of the shake table. At the same time, this dimension was realistic enough considering the dimensions of walls in practice. The thickness of the walls (10 cm) was selected considering the typical thickness of structural walls in Slovenian design practice (20 cm). The aspect ratio of the walls' cross-section was 7.5. The aspect ratio of the wall (height of the wall/ height of the cross-section) was 6. The clear distance between walls piers (see Figure 5) was 50 cm, which corresponds to the 100 cm opening in the prototype (e.g. the opening for the doors).

Figure 4. The tested specimen

The size of the slabs (3 m x 3 m) was defined following the typical tributary area for walls in RC wall buildings in Slovenia (6 m x 6 m). The thickness of the specimen's slabs (8 cm) was defined considering the typical thickness of the slab in the prototype buildings (16 cm)

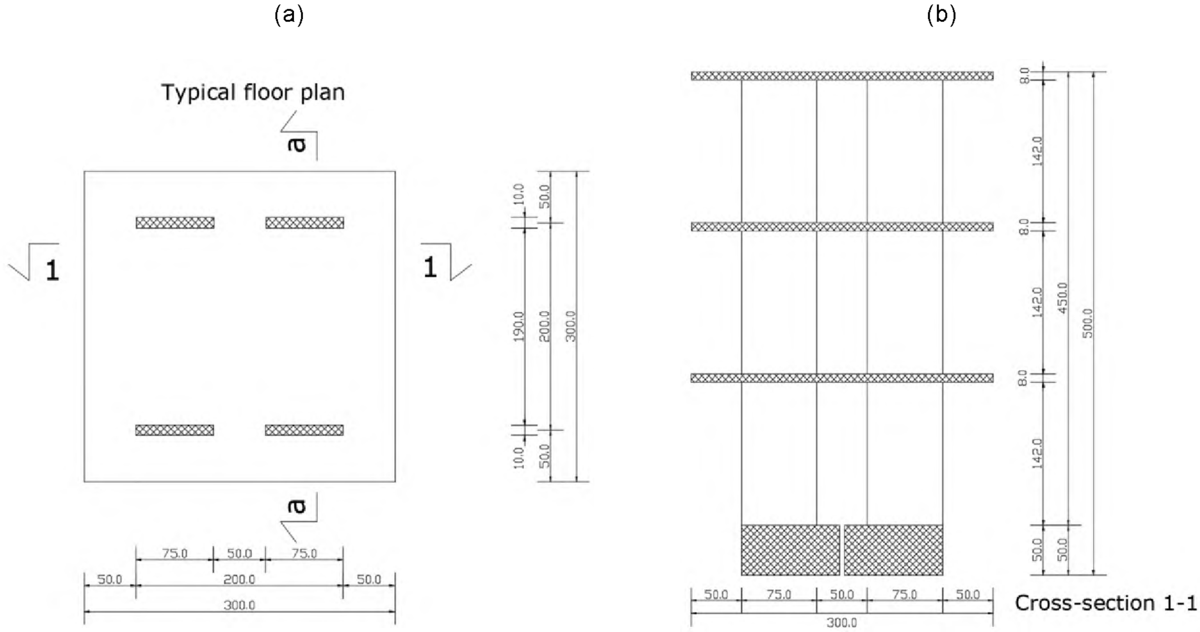

Figure 5. The specimen's dimensions and geometry: (a) floor plan, (b) side view

Table 1. Scale factors

Variable	Scale Factor Prototype/Model	Value of the Scale Factor
Length	S_L	2
Area	S_L^2	4
Volume	S_L^3	8
Moment of inertia	S_L^4	16
Mass	S_M	10
Stress	S_σ	1
Strain	1	1
Modulus of elasticity	1	1
Force	S_L^2	4
Moment	S_L^3	8
Acceleration	$S_\sigma \cdot S_L^2 / S_M$	1·4/10 = 0.4
Time	$\sqrt{S_M/S_L/S_\sigma}$	√(10/1/2) = 2.24

The total mass of the specimen without foundations was 8.2 t. In general, in most of the shake table tests, additional masses are typically provided to obtain the realistic demand. Therefore, steel ingots are often installed at the slabs. In the studied case, this was not an option since the ingots affected the main properties of the floors (strength and stiffness), which made a crucial influence on their interaction with wall piers. Instead of the added masses, the time and the accelerations were properly scaled (see Table 1) to obtain the realistic demand.

2.2 Material properties and the reinforcement

The strength of the used concrete was on average 26 MPa and 27.5 MPa for walls and slabs, respectively.

In walls, the minimum flexural (longitudinal) reinforcement was provided. Initially, it was planned to use 12 ribbed bars of diameter 6 mm. Since only the brittle bars of such diameter were available on the market, the walls were finally reinforced by 12 ductile plain bars of diameter 8 mm (see Figure 6a). The yielding and ultimate stress of the corresponding steel was 300 MPa and 420 MPa, respectively. The shear reinforcement ϕ6 mm/7.5 cm was provided over the entire height of the walls.

The slabs were reinforced by two reinforcing meshes Q-131, providing 1.31 cm^2/m for the top and the bottom reinforcing layers (see Figure 6b). The yielding and the ultimate stress of the corresponding steel were 500 MPa and 560 MPa, respectively.

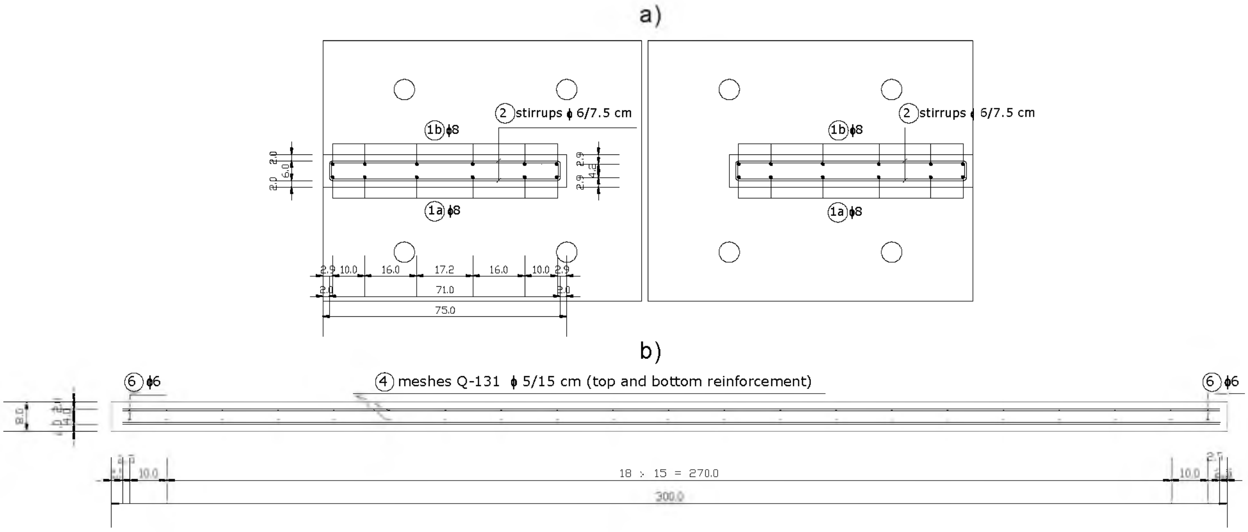

Figure 6. The reinforcement of a) walls and b) slabs

2.3 Seismic excitation

The shake table was excited by an artificial accelerogram (see Figure 7a), which was generated by modifying accelerogram Petrovac N-S, registered during the 1979 Montenegro earthquake. This accelerogram was modified to match the EC8 acceleration spectrum corresponding to soil site type A and 2% damping. The 2% damping was considered since, in most experiments, viscous damping is typically smaller than in actual buildings due to the lack of different sources of damping (e.g. partition walls, etc.). The target accelerogram and the accelerogram applied during the tests and the corresponding acceleration spectra are presented in Figure7a and 7b, respectively.

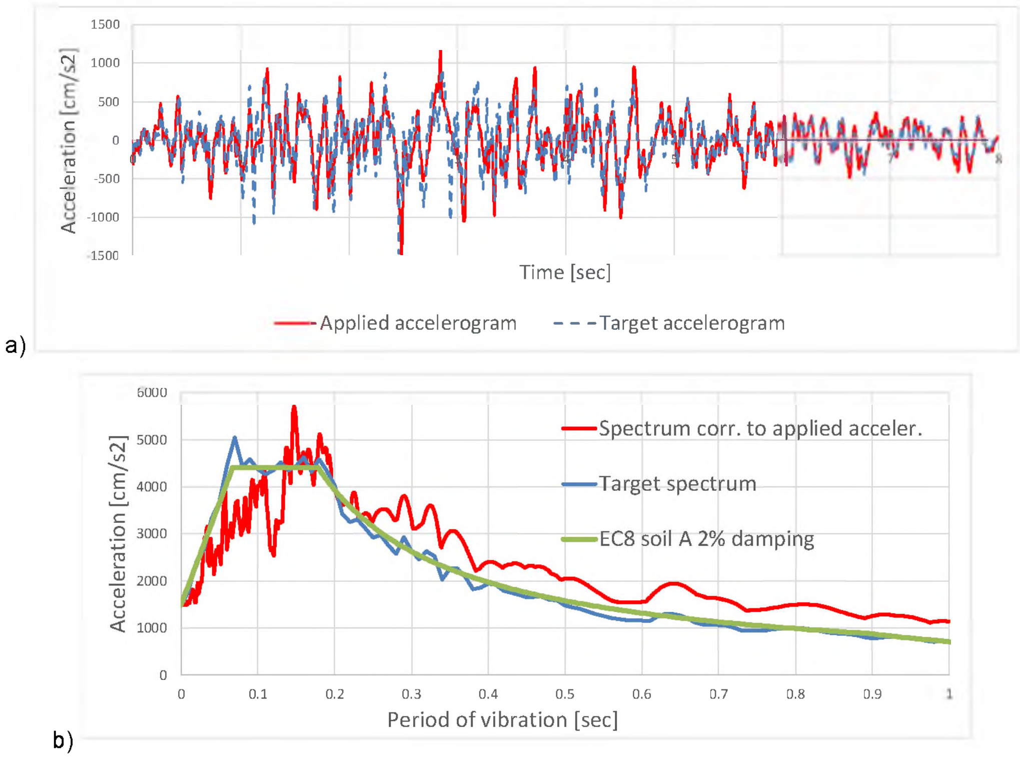

Figure 7. Seismic excitation: a) target and applied accelerogram, b) corresponding acceleration spectra for PGA = 1,5 g (Note: The time and accelerations are scaled considering the scale factors from Table 1).

A series of uniaxial tests were performed, with gradually increasing intensity of the seismic excitation in the direction of walls (N-S – see Figure 8). All runs are summarized in Table 2. The testing was concluded when the displacement capacity of the shake table was exhausted (12 cm). In between the tests, the periods/frequencies of the structure were measured. The measured values were 0.14 sec, 0.20 sec, 0.32 sec, and 0.32 sec before the first test R010, after R060(2), after R150(1), and after R150(2), respectively.

Table 2. The list of the performed tests

Test	Maximum acceleration at the shake table	Period of vibration
R010	0.1 g	0.14 s (before the test)
R020	0.2 g	
R030	0.3 g	
R050	0.5 g	
R060(1)	0.6 g	
R060(2)	0.6 g	0.20 s (after the test)
R080	0.8 g	
R090	0.9 g	
R120	1.2 g	
R150(1)	1.5 g	0.32 s (after the test)
R150(2)	1.5 g	0.32 s (after the test)

2.4 Instrumentation

The instrumentation is summarized in Figure 8.

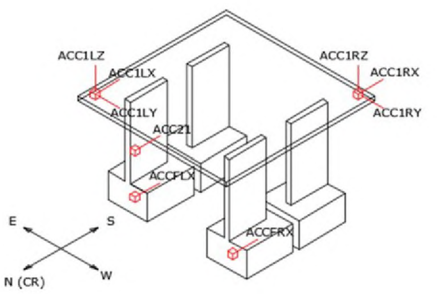

a) Accelerometers were installed at all slabs and at the foundation level (only the scheme of the first story is presented)

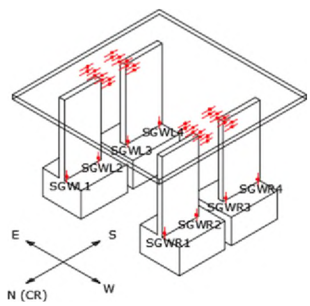

c) Strain gauges were used to measure deformations in all slabs and at the bottom of walls (only the first story is presented)

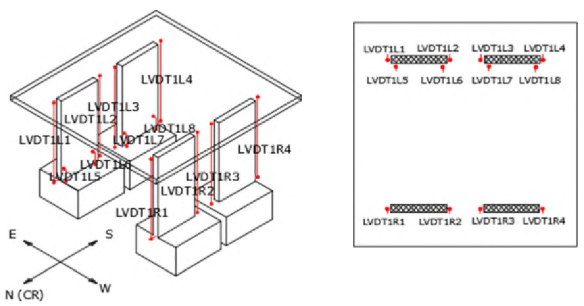

b) LVDT'S were used to measure relative vertical displacements (deformations) along all stories and at the bottom of the walls (only the first story is presented)

d) Optical measurements of deformations were performed at outer faces of the bottom story of all walls

Figure 8. An overview of the instrumentation

3 Response of the tested specimen

3.1 Observed response

The response of the tested building was essentially elastic up to the test R120. The first cracks were observed at the bottom of the wall piers and in the 1ststory slab near the joints with the walls after the test R030. When the seismic intensity was increased, the cracks also appeared in the second and the third slab. The cracks in the slabs were first limited to the area near the joints with the walls. When the seismic intensity was increased, they were gradually expanded to the whole width of the slabs between the two rows of wall piers (see Figure 9). The cracks were clearly visible at the top and the bottom surfaces of the slabs.

The damage in the wall piers was initiated at the very bottom cross-section near the foundations. Later on, additional cracks were gradually formed up to approximately 100 cm from the foundation level (see Figure 10a). The cracks were initiated at the outer edges of each wall pier.

When the seismic intensity was increased, they extended toward the inner edges (see Figure 10a). The crack pattern was considerably different from the cross-shaped damage pattern, typical for cantilever walls (compare the crack patterns, presented in Figures 10a and 10b).

In test R120, the response of the building entered the nonlinear range. The cracks were spread over the entire width of the slab in between the two rows of the wall piers (see Figure 9). The width of the cracks in the slabs was considerably increased. The yielding of the reinforcement in the slabs was achieved. The effective width of slabs was equal to their total width. The flexural strength of slabs was fully activated, generating considerable axial forces in wall piers (see Figure 1b). The frame action caused by the slabs was considerable (see also the discussion in section 3.3).

The response of two wall piers located at the same side of the specimen was considerably different. This is evident in Figure 11a, where the two piers' response (obtained with optical measurements) is presented. In the left pier, where the tensile axial force was generated, the considerable cracks were formed approximately up to 1m from the foundation level (see the orange areas surrounded by the red circle, which indicate cracks). In the right wall pier, which was subjected to compression, the damage was located mostly at the bottom of the wall.

In the last two tests (R150(1) and R150(2)), where the nonlinear deformations were noticeable, the differences in the response of two piers were visible to the naked eye. The considerable rocking of the wall subjected to the tension was observed. In the last test, the buckling of the longitudinal reinforcement at the outer edge of one of the piers was observed (see Figure 11b), indicating that this pier was subjected to relatively large compression stresses.

a) 

b) 

Figure 9. Cracks were formed a) at the top and b) at the bottom surfaces of the slabs, all over their width between two rows of wall piers

a) 

b) 

Figure 10. a) Cracks, which were observed in the wall piers,

b) Crack pattern typical for cantilever walls (courtesy of Tran and Wallace [9])

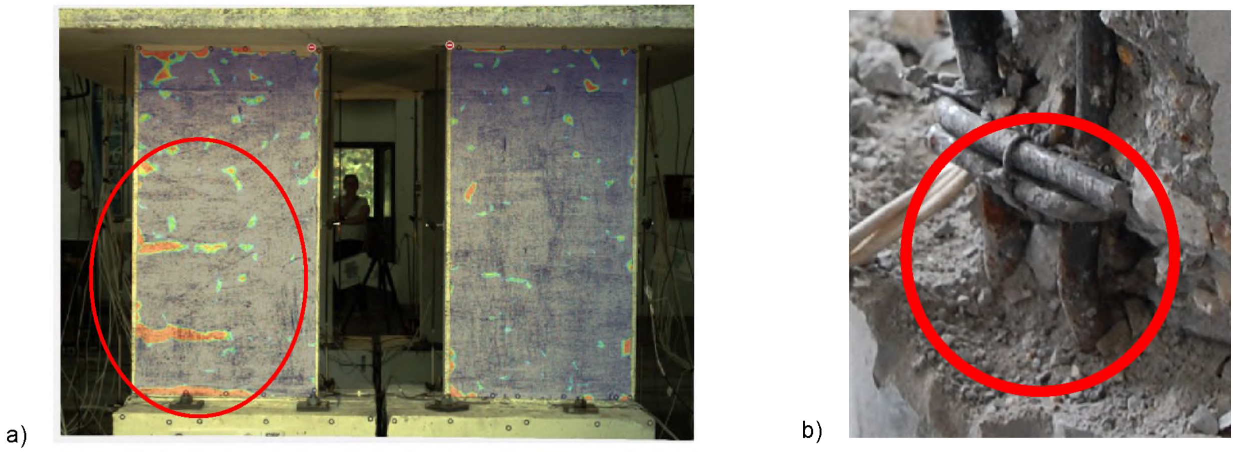

Figure 11. a) Response of two piers was considerably different, b) Buckling of the longitudinal bars was observed in the outer edge of one pier

3.2 Global parameters of the response

The envelopes of horizontal story accelerations, the envelopes of horizontal displacements and the envelopes of story drifts in the direction of the seismic excitation (N-S see Figure 8) are presented in Figure 12. The presented accelerations are the average values of the accelerations measured at two stations (see Figure 8a) at each slab. The hysteretic response throughout all tests, expressed in terms of displacements and the base shear, is presented in Figure 13. The base shear is estimated from the measured average story accelerations.

The response of the tested building was essentially elastic up to the test R120. In this test, one peak acceleration of 1.2g was registered at the shaking table. The majority of strong peaks had an intensity of 0.8g. This corresponds to the peak ground acceleration of 0.32g in the prototype structure. Note, however, that the response of structures subjected to different real accelerograms can enter the nonlinear range also at smaller peak ground accelerations. The level of yielding also depends on the geometry of the building. In higher and narrower structures (e.g. concrete cores), yielding can occur at the lower seismic intensities. This is the topic of ongoing extensive parametric study at UL FGG.

Maximum acceleration of 3.4g was registered at the top of the building at test R150(2). It corresponds to the acceleration excitation of the shake table of 1.5g. Note, however, that seismic excitation of 1.5g was applied only in one single time step (see Figure 7a). Most of the local maximums corresponded to the acceleration excitation of about 1g. This corresponds to an acceleration of 0.4g in the prototype structure (see Table 1).

During the last test, R150(2), the maximum displacement of 53 mm was obtained at the top of the building in both directions (N-S and S-N). This value corresponds to a 1.1% drift. The displacement envelope was almost linear, and the story drifts almost constant in all stories (see Figures 12b and 12c). This is an additional indication that the response was different from that typical for cantilever walls.

The top displacement to base-shear relationship, presented in Figure 13c, confirms the visual observations from the experiment that the structure entered the nonlinear range in the test R120. The gradually decreasing stiffness of the structure (see Figure 13 a-c) is in good agreement with the measured increasing periods of vibrations (see section 2.3).

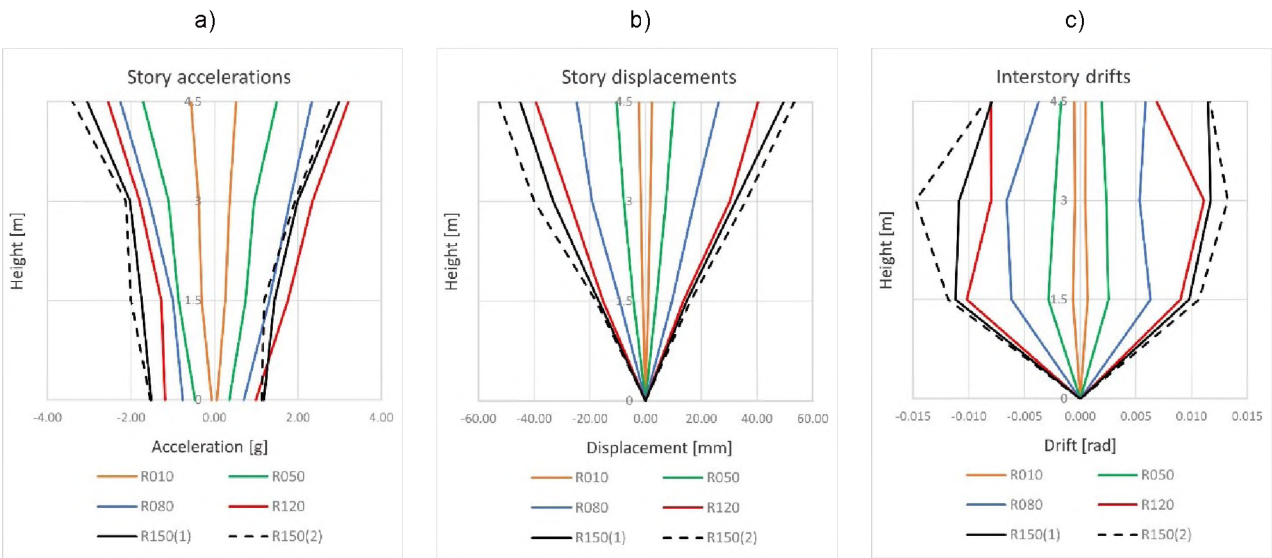

Figure 12. Envelopes of a) horizontal story accelerations, b) horizontal story displacements, c) story drifts in the direction of excitation

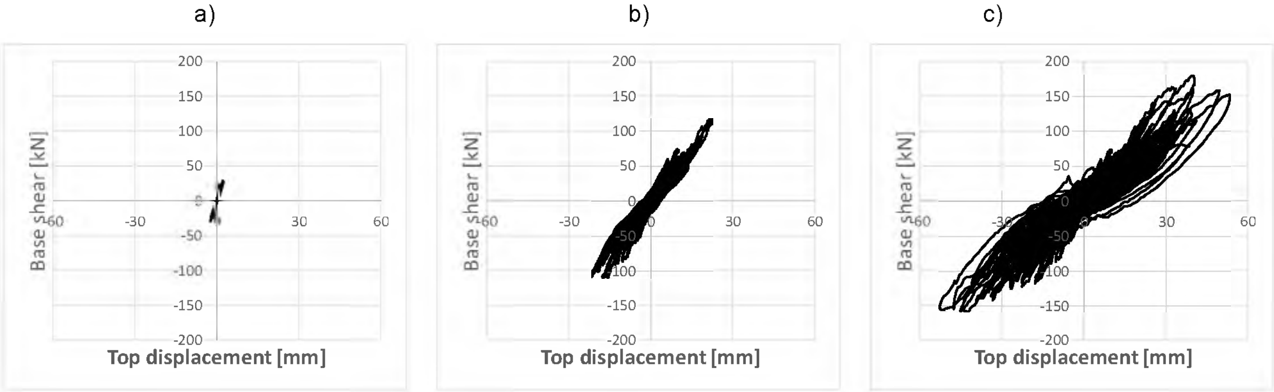

Figure 13. Hysteretic response at three different stages of testing: a) after R010, b) after R060(2), and c) after the last test R150(2)

3.3 Estimated level of coupling

The coupling level was estimated considering the ratio of the overturning moment resisted by the flexural response of piers and the shear resisted by the frame action of slabs (moment due to the axial forces in walls resulting from the accumulated shear in slabs – see Section 1).

The coupling level was analyzed considering the response of the two wall piers at the east side of the tested building (see Figure 8), which was damaged more than the west part (due to the construction imperfections, certain torsion was activated, causing some differences in the response of the east and west side of the specimen). The representative example of this analysis is provided in the following paragraphs, considering one of the peak excitations during the last test, R150(2). In this test, the yielding of wall piers was observed, and their flexural capacity was achieved.

The overturning moment was estimated based on the inertial forces, calculated at all stories from the accelerations measured at the east side of slabs (see Figure 8a) and the tributary mass (half of the mass of the tested specimen). The bending moments at the foundations level caused by these forces were summed to obtain the total overturning moment.

At the beginning of the analysis, the axial forces in piers were unknown. Thus, their flexural capacity was estimated considering the axial force caused by the gravity load N_g = 20 kN per wall pier. Both piers' corresponding total flexural capacity was M_{FC} = 140 kNm (70 kNm per wall pier).

The overturning moment M_{over} was 290 kNm. Considering the flexural capacity of piers (M_{FC} = 140 kNm), the part of the overturning moment resisted by the frame action was defined as M_{FA} = 290 – 140 = 150 kNm.

To obtain the axial forces N_E in wall piers caused by the seismic excitation, M_{FA} was divided by the axial distance of wall piers (1.25m). In this way, N_E was estimated to be 120 kN. In one wall pier, this force was tensile in the other compressive (see Figure1b).

In the next step, N_E and N_g were summed to obtain the total axial forces in piers (due to the gravity and the seismic load). In the pier subjected to tension, the axial force was N_t = 100 kN (tensile force). In pier subjected to compression, the axial force was N_c = 140 kN (compressive force).

The flexural capacity of each pier at axial load N_t and N_c was calculated to be 30 kNm and 105 kNm, in the pier subjected to tension and compression, respectively. Thus, the total flexural capacity of both piers was M_{FC} = 135 kNm. Consequently, the value of the overturning moment, resisted by the frame action, amounted to:

$$M_{FA} = M_{over} - M_{FC} = 290 - 135 = 155 \text{ kNm} \quad (1)$$

$$M_{FC}/M_{over} = 155/290 = 0.53 \quad (2)$$

Note that despite considerable changes of the axial forces in wall piers and considerable changes of their flexural capacity (compared to that corresponding to N_g), the total flexural capacity of both piers was only slightly changed. This is not surprising, considering that the flexural capacity of the piers is changing proportionally to the changes of the axial force. In pier subjected to tension, the flexural capacity was reduced. At the same time, the flexural capacity in the pier subjected to compression was increased for the approximately same amount.

In the analyzed case, the part of the overturning moment resisted by the frame action was 53 % of the total overturning moment M_{over} (see Equation 2). Note that in Eurocode 8, the coupled walls are defined as walls where the frame action contributes more than 25 % of the total overturning moment. Considering this definition, the analyzed structure should be designed following the rules for buildings with coupled walls.

As mentioned before (see Section 1), the studied walls are typically designed as cantilever walls, neglecting the frame action induced by slabs. In the studied case, this would considerably underestimate the compression stresses and shear forces in the piers subjected to compression. This could lead to brittle failure of the wall and the damage, which is similar to that observed in the recent earthquakes (e.g. buckling of the longitudinal bars, which was observed in the presented experiments).

4 Conclusions

The half-scale shake table tests of the three-story RC coupled wall building were conducted to study the slab-to-wall interaction. The specimen consisted of four rectangular walls connected only by the slabs.

A numerical model consisting of four cantilever walls connected with a rigid diaphragm would be typically used for the seismic analysis of such structures. In this way, the flexural stiffness and the strength of slabs are neglected, assuming that they are small compared to those of wall piers and insignificantly affect the response of the whole structure. This further means that it is assumed that slabs without beams cannot considerably couple wall piers.

In the experiment, contrary to this generally accepted approach, the considerable coupling of relatively flexible wall piers was provided only by slabs. The flexural capacity of slabs at the plastic hinges near the wall piers was large enough to provide strong frame action. The ratio of the overturning moment resisted by the frame action was larger than 50 %. In Eurocode 8, the upper value of this effect defining the cantilever wall systems is half of that observed in the experiment (25 %).

All slabs were fully activated. They were considerably cracked over the entire width between two rows of piers. The response of the wall piers was substantially different from that typical for the cantilever walls. The considerable rocking was observed in the piers subjected to relatively large tension induced by the frame action. In piers subjected to compression, the buckling of the longitudinal bars occurred due to the relatively large compressive stresses also caused by the frame action of the slab.

The presented experiment confirmed the indications of some other experiments found in the literature that for certain building configurations, only the slabs without beams can provide considerable coupling of wall piers. In such cases, the typical design, based on the assumptions that the walls respond as cantilever walls, can significantly underestimate the demand in piers. This can further lead either to brittle shear failure of walls or to their failure caused by the buckling of the longitudinal bars induced by significant compression stresses, which were underestimated in the design.

Acknowledgements

The project leading to this paper received funding from the European Union's Horizon 2020 research and innovation programme under grant agreement No 730900.

References

[1] M. Fischinger, P. Kante, T. Isaković, Shake-table response of a coupled RC wall with thin T-shaped piers,Jour. of Struc. Eng. 143:5, (2017) 1-16.

[2] A.R. Santhakumar,The ductility of coupled shear walls. Dissertation, University of Canterbury, (1974).

[3] R. Alvarez, J.I. Restrepo, M. Panagiotou, R.A. Santhakumar, Truss Model for analysis of reinforced concrete coupled structural walls, Bulletin of Earthquake Engineering: 17: 6419–6436, (2019).

[4] L.M. Massone, Fundamental Principles of the Reinforced Concrete Design Code Changes in Chile Following the Mw 8.8 Earthquake in 2010, Engineering Structures, vol. 56, (2013), pp. 1335-1345.

[5] Boroschek R et al., Lessons from the 2010 Chile earthquake for performance based design and code development, Performance-based seismic engineering: vision for an earthquake resilient society, Dordrecht: Springer, (2014), pp 143 – 157.

[6] K.J. Elwood et al., Performance-Based Issues from the 22 February 2011 Christchurch Earthquake, Performance-based seismic engineering: vision for an earthquake resilient society. Dordrecht: Springer, (2014), pp 159 – 175.

[7] M.M. Panagiotou et al., Shake-Table Test of a Full-Scale 7-Story Building Slice. Phase I: Rectangular Wall, Jour. of Struc. Eng., 137: 6, (2011).

[8] T. Nagae, K. Tahara, T. Matsumori, H. Shiohara, T. Kabeyasawa, S. Kono, M. Nishiyama, J. Wallace, W. Ghannoum, J. Moehle, R. Sause, W. Keller, Z. Tuna Z, Design and Instrumentation of the 2010 E-Defense Four-Story Reinforced Concrete and Post-Tensioned Concrete Buildings, PEER Report 2011/104,Pacific Earthquake Engineering Research, Berkeley, USA, (2011).

[9] T.A. Tran, J.W. Wallace, Cyclic Testing of Moderate-Aspect-Ratio Reinforced Concrete Structural Walls,ACI Structural Journal 112(6)(2015), pp.653-665.